Observation of ac Stark-effect-enhanced four-wave mixing in a near-resonant four-level system

Chen-Yu Tai, Charles C. Kim, R. T. Deck, and Yet-Ta Wu
Department of Physics and Astronomy, University of Toledo, Toledo, Ohio 43606
(Received 4 October 1985; revised manuscript received 16 January 1986)

Two laser beams at frequencies ν_1 and ν_2 are used to produce nonlinear scattering (wave mixing) in I_2 vapor at frequency $2\nu_1+\nu_2$. The scattering results from near-resonant allowed transitions in I_2 molecules and is observed to be anomalously strong when both laser beam frequencies are detuned in the *same* direction from frequencies corresponding to resonance in the free molecule. The strong scattering is interpreted in terms of a resonantly enhanced ac Stark shift caused by a configuration interaction between the "dressed molecular levels." By tuning the two pulses simultaneously, a tuning range of approximately 2 Å (50 cm^{-1}) is achieved in the mixed wave. The scattering process should therefore have practical application in the efficient generation of tunable coherent radiation in the ultraviolet and vacuum-ultraviolet range of the spectrum. Some of the spectroscopic properties of the three-quantum state at $E\sim 53\,000$ cm^{-1} are studied.

I. INTRODUCTION

The ac Stark shift[1] of atomic levels is one of the fundamental atomic parameters in the interaction of light and matter. The effect of the shift on the state of a two-level atomic system has been widely studied in spontaneous emission[2–4] and absorption to a third level[5] as well as in stimulated processes.[6] Recently, parametric amplification utilizing the nonlinear response of a two-level system has been shown[7,8] to lead to the generation of tunable radiation in the visible region of the spectrum. In contrast the ac Stark effect in a four-level system has received little attention. Here we report the observation of an apparent ac Stark-effect-enhanced nonlinear scattering (wave mixing) in a four-level system derived from the vibronic rotational states of the iodine molecule.

The ac Stark effect in a four-level system has some interesting characteristics as compared with the case in a two-level system. As an example, in the case of a two-level system the main peak in the coherent scattering spectrum has the same frequency ω as that of the input laser beam and may not be easily detected. For this reason the side bands at frequencies $\omega+\Omega$ (where Ω is the generalized Rabi frequency) are often the main object of interest. In a four-level system, the main peak of the nonlinear scattering has a frequency $(2\omega+\omega')$ different from that of the input light at frequency ω and ω' and can be detected directly. Resonance in the nonlinear scattering in a nearly resonant four-level system is believed to be caused by the interfering and mixing of the energy levels of the system which is composed of the molecule and the field (or "dressed molecular levels"[9]). This is similar to the configuration interaction of atomic and molecular energy levels in the conventional antilevel crossing spectroscopy.

Resonant wave mixing in a nearly resonant four-level system may also have practical application in the efficient generation of tunable coherent ultraviolet and vacuum-ultraviolet light. As compared to the method of uv light generation by two quantum resonant wave mixing in an atomic vapor with an additional resonance in an autoionizing state,[10] the method described here allows for a wider range of tunability with approximately constant output, and may also result in a higher ultimate conversion efficiency. Resonant wave mixing in atomic vapor is generally limited by saturation and has a maximum conversion efficiency of approximately 10^{-3}–10^{-2}. Because the process described here involves no exact resonance, saturation effects may be less serious.

Specifically in the process considered here two tunable dye laser beams with frequencies ω_1 and ω_2 are used to achieve near resonance in I_2 vapor. With the two beams incident on the vapor the nearly resonant vibronic rotational states of the I_2 molecule can be modeled by a four-level system. The energy levels of this system are depicted in Fig. 1 for different strengths of interaction between the molecule and the laser field, with the levels of the free molecule denoted $|0\rangle$, $|1\rangle$, $|2\rangle$, and $|3\rangle$. We define four detuning parameters in terms of the frequency differences between the latter levels and the frequencies of the two laser beams as follows:

$$\frac{\Delta_1}{\hbar}=\Omega_1-\omega_1,\quad \frac{\Delta_2}{\hbar}=\Omega_2-2\omega_1\ ,$$

$$\frac{\Delta_3}{\hbar}=\Omega_3-\Omega_2-\omega_2,\quad \frac{\delta}{\hbar}=\Omega_3-2\omega_1-\omega_2\ .$$

Here δ represents the detuning of the combined beams from resonance with the overall transition and is expressible as $\delta=\Delta_3+\Delta_2$. In a resonant wave mixing process in the absence of an ac Stark shift, the scattered signal at frequency $2\omega_1+\omega_2$ is expected to be maximized for $2\omega_1+\omega_2=\Omega_3$ or $\delta=0$. In contrast, in the presence of the Stark effect, we find the signal at $2\omega_1+\omega_2$ to be maximized when both the detunings Δ_2 and Δ_3 have the *same sign,* and δ is therefore appreciably different from zero. This means that resonance in wave mixing is observed where the incident beams are not in resonance with either

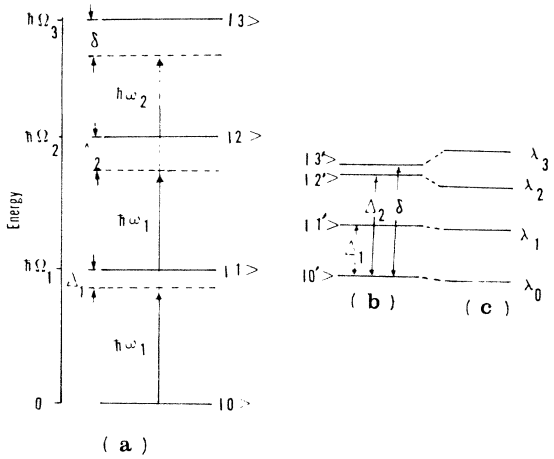

FIG. 1. Energy-level diagram for system considered. (a) Energy levels of free molecule shown in relation to laser photon energies. (Size of the detunings Δ_1, Δ_2, and δ is exaggerated.) (b) Particular set of energy levels of the total system of molecule and laser field in the absence of interaction. (c) Energy levels of the total system in the presence of the ac Stark interaction.

the one, two, or three quantum transitions. As a result a large output signal can be obtained for frequencies in an appreciable range on either side of Ω_3, and therefore, the mixed wave signal can be tuned over a significant range.

The technique of achieving resonance in one and two quantum transitions simultaneously with a single laser beam has been discussed before.[11] In Fig. 2 the transition

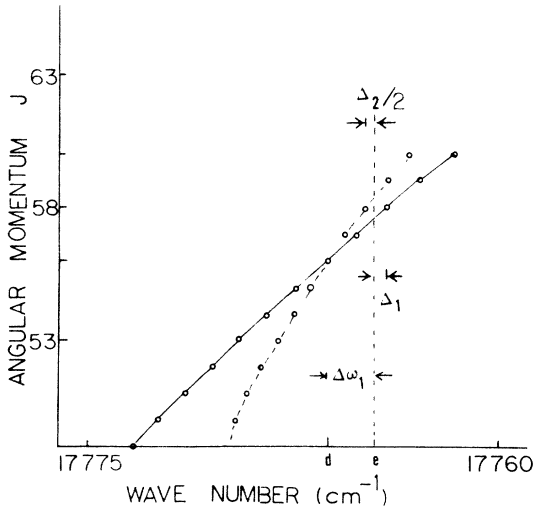

FIG. 2. Curves determining the energies (in terms of wave number) of the $|0\rangle$-$|1\rangle$ and $|0\rangle$-$|2\rangle$ transitions in the I_2 molecule for different angular momentum values J. The solid and dashed curves graph, respectively, the wave number (versus J) of the $|0\rangle$-$|1\rangle$ transition and one-half the wave number (versus J) of the $|0\rangle$-$|2\rangle$ transition. At the wave number (value d) corresponding to the crossing point of the two curves the laser is tuned to be simultaneously resonant with the one and two quantum transitions in molecules with angular momentum $J=56$. At the wave number (value e) shifted from the value d by approximately 50 GHz, the laser is detuned from resonance with both the one and two quantum transitions in molecules with $J=58$ by only about 12 GHz.

frequency of the one quantum transition, $|0\rangle$-$|1\rangle$, and half the frequency of the two quantum transition $|0\rangle$-$|2\rangle$, in a particular vibrational band are plotted separately as abscissa versus the angular momentum J of the molecule in its ground state. The condition of simultaneous resonance in the $|0\rangle$-$|1\rangle$ and $|1\rangle$-$|2\rangle$ transition is satisfied for a molecule which has the value of angular momentum corresponding to the intersection of the two plots ($J=56$ in the diagram). It can be seen that, even with the frequency of the laser light detuned from the frequency corresponding to the "double resonance," there is a wide range of frequency for which the detunings from the two resonances corresponding to some particular angular momentum value are relatively small. For example, at the frequency $\nu(e)$, shifted from the frequency $\nu(d)$ by 50 GHz, the detunings from the two resonances for a molecule with $J=58$ in its ground state are each only about 12 GHZ. As a result, a laser beam with an appropriate frequency and an intensity such that the Rabi frequencies for the transitions $|0\rangle$-$|1\rangle$ and $|1\rangle$-$|2\rangle$ have values of several GHz can induce molecular transitions between the $|0\rangle$ and $|2\rangle$ levels efficiently over a wide range. If this beam is combined with a second laser beam tuned to be in near resonance with a transition from level $|2\rangle$ to a third excited level $|3\rangle$, the combined beams can result in efficient excitation of level $|3\rangle$ and consequently production of coherent uv radiation corresponding to the transition $|3\rangle$-$|0\rangle$. Previous work based on comparison of the input power dependence of triply resonant wave mixing and that of doubly resonant third harmonic generation indicates that a moderately focused beam with an intensity of 2 mJ/pulse (pulse duration ~ 16 ns) and a linewidth of 10 GHz has Rabi frequencies of approximately 2 GHz (Ref. 12) in I_2 vapor and is suitable for efficient generation of uv radiation via a triply near resonant process with two beams.

In this work the experimental result on near-resonant nonlinear scattering will be discussed first. A qualitative comparison with the prediction of a simplified semiclassical theory which assumes the Rabi frequencies small as compared to the laser frequency detuning will then be discussed. A general theory which applies to the case that the Rabi frequencies are comparable to or larger than the detunings is complicated and will be presented in another paper. Effects of damping on the intensity and shifting of the resonant nonlinear scattering are interesting but complicated and will also be neglected in this work.

II. EXPERIMENT

The experimental setup of this work is shown in Fig. 3. A Molectron DL-II dye laser pumped by a Molectron MY-32 Nd:YAG (neodymium-doped yttrium aluminum garnet) laser provides 16-ns pulses for two-photon excitation of the $|0\rangle$-$|2\rangle$ transition in the I_2 molecule. The bandwidth of the beam is approximately 0.1 cm^{-1} and the power is approximately 3 mJ/pulse. By use of a 50-cm focal length lens the beam is focused to a cross section of approximately 0.1 mm^2 at the center of a 1-cm-long cell containing pure I_2 vapor at room temperature (vapor pressure ~ 0.3 Torr). The wavelength of this beam is tuned to

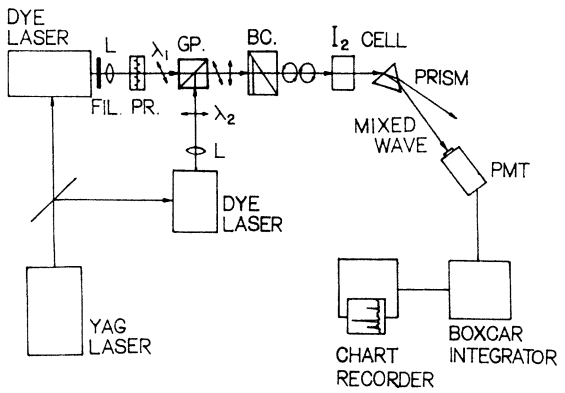

FIG. 3. Diagram showing arrangement of apparatus used in observation of near-resonant wave mixing process. Beams from dye lasers 1 and 2 are combined collinearly via a Glan prism (GP), and converted into two oppositely circularly polarized beams by adjusting of the compensator (BC) for $\lambda/4$ retardation. After passage of the combined beams through the I_2 cell the high-frequency mixed-wave signal is detected by a uv sensitive photomultiplier tube (PMT), averaged by a boxcar integrator and recorded on a chart recorder. In the first part of the experiment the wavelength of beam 1, $\lambda(1)$, is fixed at a value near that which produces a maximum in the third harmonic signal and the wavelength of beam 2, $\lambda(2)$, is scanned to find a maximum in the mixed-wave output.

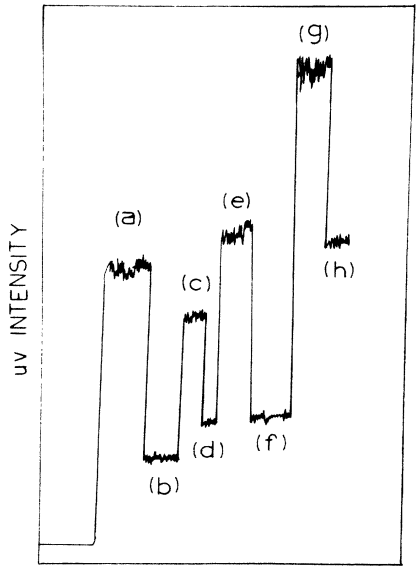

FIG. 4. Intensity of the mixed-wave signal for various wavelengths $\lambda(1)$ and $\lambda(2)$ of the incident laser beams. (a) $\lambda(1)$ tuned to be simultaneously resonant with the $|1\rangle$-$|0\rangle$ and $|2\rangle$-$|1\rangle$ transitions and $\lambda(2)$ tuned to be resonant with the $|3\rangle$-$|2\rangle$ transition. (b) $\lambda(1)$ detuned by 0.1 Å from case (a), $\lambda(2)$ unchanged. (c) $\lambda(1)$ detuned by 0.1 Å from case (a), $\lambda(2)$ detuned by 0.3 Å from case (a). (d) $\lambda(1)$ detuned by 0.1 Å from case (c), $\lambda(2)$ unchanged from case (c). (e) $\lambda(1)$ detuned by 0.1 Å from case (c), $\lambda(2)$ detuned by 0.2 Å from case (c). By continuation of the process of adjustment of $\lambda(1)$ and $\lambda(2)$, a large mixed-wave signal can be obtained over a tuning range (in the output) of approximately 2 Å.

give maximum third harmonic in the vicinity of 5630 Å so that the beam is resonant with transitions $|0\rangle$-$|1\rangle$ and $|1\rangle$-$|2\rangle$ simultaneously with the compensator BC shown in the diagram adjusted for zero retardation. A second laser beam of wavelength $\lambda(2)$ is combined collinearly with the first beam by means of a Glan prism and focused in the sample cell by means of a 40-cm focal length lens to approximately the cross section of the first beam. The second beam is provided by a National Research Group DL03 dye laser pumped by the same Nd:YAG laser. It has an intensity of approximately 40 μJ/pulse and a bandwidth at half maximum of about 0.7 Å (with an intensity decreasing slowly to zero outside the central band). Background third harmonic radiation produced by either beam separately is eliminated by conversion of the two linearly polarized beams into oppositely circularly polarized beams via adjustment of the compensator for quarter wave retardation. The mixed wave at frequency $2\nu_1+\nu_2$ is separated from the laser beams by a prism, filtered by two narrow band uv interference filters and detected by a uv sensitive tube (EMI G-26G-315). The output signal is averaged by a boxcar integrator and displayed on a chart recorder. A strong resonance in the mixed wave is observed when the second beam is tuned to a resonance in the $|2\rangle$-$|3\rangle$ transition. A discussion of the spectrum of the mixed wave as well as its input power dependence will be given in another paper. Here we will concentrate on how the intensity of the signal depends on the wavelength of the two input laser beams with $\lambda(1)$ tuned in the vicinity of 5630 Å and $\lambda(2)$ tuned in the vicinity of 5787 Å.

In Fig. 4(a) we plot (in arbitrary units) the intensity of the uv radiation detected versus the wavelength of laser beam 2 with the wavelength of laser 1 tuned to a set of different values in the vicinity of the resonance value for the transitions $|0\rangle$-$|1\rangle$ and $|1\rangle$-$|2\rangle$. Figure 4(a) shows the uv intensity in the case that $\lambda(1)$ is tuned to simultaneous resonance with the $|0\rangle$-$|1\rangle$ and $|1\rangle$-$|2\rangle$ transitions and $\lambda(2)$ tuned to resonance with the transition $|2\rangle$-$|3\rangle$. With $\lambda(2)$ fixed at this resonance value, Fig. 4(b) shows the decreased value of the uv intensity resulting from an increase in the value of $\lambda(1)$ by 0.1 Å. With $\lambda(1)$ fixed at this detuned value, Fig. 4(c) shows that the uv intensity is again increased when the wavelength $\lambda(2)$ is also detuned from its resonance value by an increase of about 0.3 Å. Parts (d)—(h) of Fig. 4 show the results of continuing the process of increasing first $\lambda(1)$ and then $\lambda(2)$ so as to decrease and then increase the output uv intensity. This process allows high-intensity uv radiation to be obtained over a tuning range of more than 4 Å in $\lambda(1)$ and 6 Å in $\lambda(2)$. Interestingly, the highest-intensity uv radiation is generated for detunings in the wavelengths $\lambda(1)$ and $\lambda(2)$ which are both nonzero and of the *same sign*. As a consequence the maximum in the uv light generated in this process has a tuning range of over 50 $cm^{-1}\sim 2$ Å (the precise range being somewhat a function of the input power). Since the I_2 cell is optically thin and the optical path is much shorter than the coherence length (~ 5 cm), this phenomena can not be explained in terms of an increase in the coherence length.

The intensity of the uv radiation measured as a function of the wavelength of the second beam for a set of values of the wavelength of the first beam is shown in Fig. 5. The power of the first beam is fixed at 2.5 mJ/pulse. It is tempting to interpret the two peaks shown in each of the separate plots in terms of the P and R branches of some vibrational band of the $|3\rangle$-$|0\rangle$ transition, but as will be explained below, this interpretation appears incorrect. Figure 5 indicates again that the maximum uv radiation is generated where the detunings of $\lambda(1)$ and $\lambda(2)$ from their free molecular resonance values are both nonzero, and that as the detuning in $\lambda(1)$ is increased, the uv radiation is maximized only when the detuning in $\lambda(2)$ is also increased.

The uv intensity at the maximum of the two peaks shown in Fig. 5 is plotted in Fig. 6 as a function of the wavelength of the first beam for two different beam 1 input powers of 2.5 and 0.6 mJ/pulse, respectively. Maximum intensity in the nonlinearly scattered (mixed) wave seems to be periodic in the wavelength of beam 1 with a period roughly equal to the separation between resonances associated with adjacent J values. A comparison of Figs. 6(a) and 6(b) indicates that the variation in the intensity of the uv light decreases with the input power of beam 1. Fig. 6(c) shows the intensity of the third harmonic generated by beam 1 alone when it is linearly polarized and has an intensity of 0.6 mJ/pulse. Comparison of parts (a) and (c) of Fig. 6 indicates that the uv light generated in nearly resonant wave mixing can have a much larger tunable range as compared with the technique of third harmonic generation. The magnitude of the peak uv intensity generated in the near resonant wave mixing process is surprising, as is the common sign of the detuning in $\lambda(1)$ and $\lambda(2)$ required to produce the peak in the wave mixing.

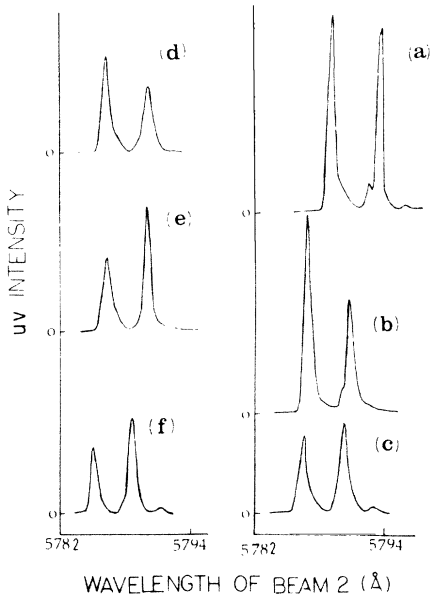

FIG. 5. Intensity of the mixed-wave signal versus the wavelength $\lambda(2)$ of beam 2 for a set of values of $\lambda(1)$, with the power of beam 1 fixed at 2.5 mJ/pulse. λ_d corresponds to crossing point of the curves of Fig. 1. (a) $\lambda(1)=\lambda_d+1.7$Å, (b) $\lambda(1)=\lambda_d+0.3$ Å, (c) $\lambda(1)=\lambda_d+0.1$ Å, (d) $\lambda(1)=\lambda_d$, (e) $\lambda(1)=\lambda_d-0.2$ Å, (f) $\lambda(1)=\lambda_d-0.8$ Å. Plots indicate that the intensity of the mixed-wave signal is largest when the wavelengths of both beams are detuned in the same direction from the values corresponding to resonances in the free molecule. The mechanism responsible for the *two* peaks is not well understood.

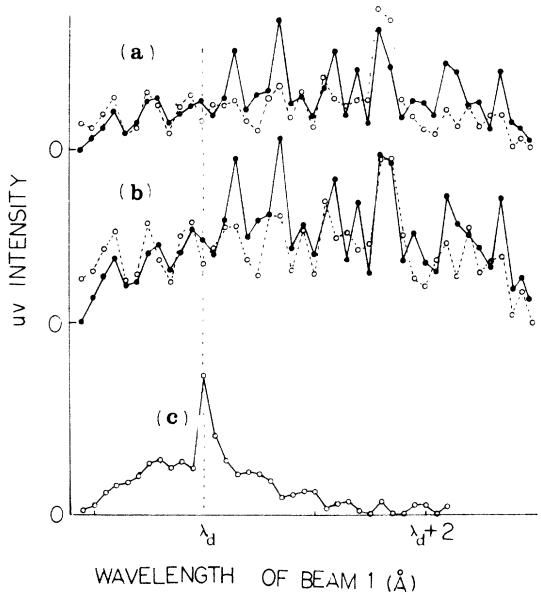

FIG. 6. Intensity of the mixed-wave signal at its maximum as a function of $\lambda(2)$ versus the wavelength $\lambda(1)$ of beam 1. The closed (●) and open (○) circles represent, respectively, the values corresponding to the first and second peaks in Fig. 5. The input power of beam 1 is 0.6 mJ/pulse in the case of curves (a) and 2.5 mJ/pulse in the case of curves (b). For comparison, curve (c) shows the intensity of the third harmonic radiation generated by beam 1 alone when it is linearly polarized and has a power of 0.6 mJ/pulse. The verticle scales for the three sets of curves are different.

III. THEORY AND DISCUSSION

In order to discuss the mechanism of resonant nonlinear scattering in a nearly resonant four-level system it is instructive to consider the energy-level diagram of the four-level molecule shown in Fig. 1. The nondegenerate levels $|0\rangle$, $|1\rangle$, $|2\rangle$, and $|3\rangle$ have energies 0, $\hbar\Omega_1$, $\hbar\Omega_2$, and $\hbar\Omega_3$. The electric field associated with the two laser beams at time t and position $\mathbf{r}$ is described by

$$\mathbf{E}(\mathbf{r},t)=\mathbf{E}_1(\mathbf{r},t)+\mathbf{E}_2(\mathbf{r},t)\ . \tag{1}$$

Here

$$\mathbf{E}_i(\mathbf{r},t)=\mathscr{E}_i(\mathbf{r},t)\exp(-i\omega_i t+\mathbf{k}_i\cdot\mathbf{r})+\text{c.c.},\quad i=1,2\ . \tag{2}$$

The amplitude functions $\mathscr{E}_i(\mathbf{r},t)$ can be assumed to be slowly varying functions of t which change only slightly in the time interval $1/\omega_i$, and for simplicity it is assumed that the electric field can be taken to be linearly polarized in the x direction. In the current experiment, the beams are circularly polarized but this makes no fundamental difference in the theory. Since the generated wave is

much weaker than the input beams, its field is neglected in the above formula. With near resonance in all three allowed transitions, the detunings of the two laser frequencies from resonances in the free molecule can be written as $\Delta_1/\hbar=\Omega_1-\omega_1\ll\omega_1$, $\Delta_2/\hbar=\Omega_2-2\omega_1\ll\omega_1$ and $\delta/\hbar=\Omega_3-2\omega_1-\omega_2\ll\omega_1,\omega_2$. In this work we will hold Δ_1 and Δ_2 at constant values and vary δ to find the maximum in the nonlinear scattering.

The time evolution of the wave function of the molecule is determined by the equation

$$\frac{d\psi(t)}{dt}=-i\hbar^{-1}(H_0+V)\psi(t)\ . \tag{3}$$

Here H_0 is the Hamiltonian for the unperturbed molecule and V is the molecule-field interaction potential defined by

$$V=-\mathbf{p}\cdot\mathbf{E}\ , \tag{4}$$

where $\mathbf{p}$ is the dipole moment operator. The matrix elements of this operator are represented as

$$p_{ij}=\left\langle i\left|\frac{\mathbf{P}\cdot\mathbf{E}}{E}\right|j\right\rangle\ . \tag{5}$$

We take the basis vectors $|i\rangle$ to correspond to the four time-independent eigenstates of H_0 shown in the diagram of Fig. 1(a). Equation (3) can be simplified by re-expressing it in terms of an interaction picture wave function $\psi_\omega(t)$, defined by

$$\psi_\omega(t)=e^{iAt}\psi(t)\ , \tag{6}$$

with

$$A=\begin{bmatrix}0&0&0&0\\0&\omega_1&0&0\\0&0&2\omega_1&0\\0&0&0&2\omega_1+\omega_2\end{bmatrix}\ . \tag{7}$$

The equation for $\psi_\omega(t)$ then becomes

$$\frac{d\psi_\omega(t)}{dt}=-i\hbar^{-1}H_\omega\psi_\omega(t)\ , \tag{8}$$

where

$$H_\omega=e^{iAT}(H_0+V-\hbar A)e^{-iAt}\ . \tag{9}$$

By use of the familiar rotating-wave approximation to eliminate the rapidly oscillating antiresonance terms, H_ω can be reduced to

$$H_\omega=\begin{bmatrix}0&a^*&0&0\\a&\Delta_1&b&0\\0&b&\Delta_2&c\\0&0&c&\delta\end{bmatrix}\ . \tag{10}$$

Here $a=-p_{10}\mathscr{E}_1\exp(i\mathbf{k}\cdot\mathbf{r})$, $b=-p_{21}\mathscr{E}_1\exp(i\mathbf{k}\cdot\mathbf{r})$, and $c=-p_{32}\mathscr{E}_2\exp(i\mathbf{k}\cdot\mathbf{r})$. Since H_ω is now time independent, Eq. (8) can be easily integrated to give

$$\psi_\omega(t)=\exp(-i\hbar^{-1}H_\omega t)\psi_\omega(t_0)\ . \tag{11}$$

The evaluation of Eq. (11) can be simplified by diagonalization of the matrix H_ω. In the limiting case of extremely weak fields E_1 and E_2, $a\sim b\sim c\sim 0$ and the eigenvalues reduce to

$$\lambda_0^{(0)}=0,\ \lambda_1^{(0)}=\Delta_1,\ \lambda_2^{(0)}=\Delta_2,\ \lambda_3^{(0)}=\delta\ . \tag{12}$$

In the case of weak pumping beams, the system of light and molecule has groups of levels at energy 0, $\hbar\Omega_1-\hbar\omega_1=\Delta_1$, $\hbar\Omega_2-2\hbar\omega_1=\Delta_2$, and $\hbar\Omega_3-2\hbar\omega_1-\hbar\omega_2=\delta(+n\hbar\omega_1+n'\hbar\omega_2)$, as shown in Fig. 1(b). As the light intensity increases, the molecule-field interaction V can no longer be neglected and these "dressed molecular energy levels" are shifted by the ac Stark effect as shown in Fig. 1(c). Assuming $\Delta_1,\Delta_2,\delta\gg|a|,|b|,>|c|$, one has

$$\lambda_0\cong\frac{a^*a\Delta_2\delta}{b^*b\delta+c^*c\Delta_1-\Delta_1\Delta_2\delta}\ , \tag{13a}$$

$$\lambda_1\cong\Delta_1+\frac{a^*a}{\Delta_1}-\frac{b^*b}{\Delta_2-\Delta_1}\ , \tag{13b}$$

$$\lambda_2\cong\Delta_2-\frac{b^*b\lambda_2(\delta-\lambda_2)+cc^*\lambda_2(\Delta_1-\lambda_2)+a^*ac^*c}{\lambda_2(\Delta_1-\lambda_2)(\delta-\lambda_2)+a^*a(\delta-\lambda_2)}\ , \tag{13c}$$

$$\lambda_3\cong\delta-\frac{cc^*\lambda_3(\Delta_1-\lambda_3)+a^*ac^*c}{\lambda_3(\Delta_1-\lambda_3)(\Delta_2-\lambda_3)-b^*b\lambda_3-a^*a(\Delta_2-\lambda_3)}\ . \tag{13d}$$

Because the eigenvalues occur on both sides of formulas (13c) and (13d), these formulas are valid even when a and b are not small as compared to Δ_1, Δ_2, and δ. In general the shifts $\lambda_i-\lambda_i^{(0)}$ of the eigenvalues of H_ω from their weak field values are small. However, because of the energy denominators in the above formulas, the shifts of the dressed levels $|2'\rangle$ and $|3'\rangle$ are resonantly enhanced and this can significantly affect the tuning of the laser beams required for resonant nonlinear scattering.

Evaluation of the eigenvalues allows the eigenvectors S of H_ω to be determined from the relation $SH_\omega=\lambda S$. Equation (11) can then be used to calculate the nonlinear dipole moment $P(2\omega_1+\omega_2)=\rho_{30}d_{03}+\text{c.c.}$, which determines the intensity of the scattering at frequency $2\omega_1+\omega_2$. For given Δ_1 and Δ_2 this quantity can be shown to have a peak value when the ac Stark shift, $\lambda_3-\delta$, of state $|3'\rangle$ has a maximum value and states $|3'\rangle$ and $|2'\rangle$ have a maximum mixing. A straightforward calculation shows that the maximum shift in state $|3'\rangle$ occurs for a value of δ given approximately by $\delta=\Delta_2+b^*b/(\lambda_3-\Delta_1)$ which reduces to $\Delta_2+b^*b/(\Delta_2-\Delta_1)$ when Δ_2 is much larger than $|b|$. As a result the detuning of the second laser $\Delta_3=\delta-\Delta_2\cong\delta-\lambda_3\cong b^*b/(\Delta_2-\Delta_1)$, has the same sign as the detuning of the first beam, $\Delta_1\sim\Delta_2/2$, at the peak of the mixed wave scattering. Neglecting damping, it can also be shown that the resonance in the ac Stark shift $\lambda_3-\delta$ has a linewidth of approximately $|c|$, which is the approximate value of the shift at its maximum. At small detuning of $\lambda(1)$ from λ_d the ac Stark shift of level $|3\rangle$ produced by the first beam may be mostly responsible for the detuning of the second beam. Since the resonance in

the wave mixing is apparently caused by the ac Stark effect the mixed wave is expected to disappear whenever the laser beams are turned off. The wave mixing can therefore be interpreted as scattering (similar to Raman scattering) rather than as fluorescence.

A few words should be said about the properties of the three quantum state $|3\rangle$. The experimentally observed fact that $\Delta\lambda(2)\simeq 1.5\Delta\lambda(1)$ at large $\Delta\lambda(1)$ indicates that the transition frequency $\Omega_3-\Omega_2$ decreases with increasing J values as does the transition frequency $\Omega_1-\Omega_0$ shown in Fig. 1. This suggests that the rotational constant of state $|3\rangle$ is less than that of state $|2\rangle$. The rotational constant $B(3)\sim 0.012$ cm^{-1} of state $|3\rangle$ can be determined from the relation $\Delta\nu=\Delta B(J'(J'+1)-J(J+1))$, where $\Delta\nu$ is the detuning of the second beam corresponding to $\Delta\lambda(2)\sim 1.8$ Å, $J\sim 56$, $J'\sim 60$, and $\Delta B=B(2)-B(3)$. The average intermolecular distance determined from the computed value of $B(3)$ is approximately 5 Å. This B value, however, is not consistent with the value of $B(3)\sim 0.04$ cm^{-1} derived by assuming that the two resonances of Fig. (5) belong to the P and R branches of a vibrational band. It may be reasonable to identify the three quantum state as the state D which has been studied with the conventional spectroscopic technique involving excitation of the I_2 molecule with several light sources of wavelength less than 1900 Å,[13] which technique gives the inconsistent values $R\simeq 4.63$, 3.64, 4.1, and 3.8 Å for the distance between the iodine atoms where the internuclear potential is a minimum. Since the values of R derived by the conventional technique are inconsistent with one another, the coherent technique developed in this work may be valuable in the determination of the properties of the state D. If one accepts the B value of 0.012 cm^{-1} determined directly from the J dependence of the $|3\rangle$-$|2\rangle$ transition, the two scattering peaks in Fig. 5 cannot be interpreted as the P and R branches of a vibrational structure since this interpretation leads to a B value of 0.04 cm^{-1}. Since the state responsible for the two resonances have similar properties (rotational and vibrational constants as well as symmetry), the connection between them is interesting but not well understood.

It should be remarked that maximum mixing between state $|0'\rangle$ and $|3'\rangle$ at $\delta\sim 0(\Delta\lambda(2)\sim -2\Delta\lambda(1)$ at small $\Delta\lambda(1)$ will also maximize the nonlinear dipole moment $P(2\omega_1+\omega_2)$. However, in the current experiment no strong uv light signal is detected for a detuning $\Delta\lambda(2)=-2\Delta\lambda(1)$. Since the transition from state $|0\rangle$ to $|3\rangle$ is allowed by energy conservation for this detuning, the resonance in this case may be mainly responsible for fluorescence. Resonant enhancement of the scattering for the case that states $|1'\rangle$ and $|3'\rangle$ are nearly degenerate is also predicted and may also contribute to the signal detected in our experiment.

IV. CONCLUSION

In conclusion we have observed strong resonance in the nonlinear scattering produced by a nearly resonant four-level system. The resonances are interpreted in terms of resonantly enhanced ac Stark shifts caused by the configuration interaction of the "dressed molecular levels." Because the main scattering peak corresponds to a frequency $2\nu_1+\nu_2$, which is different from the frequencies of the primary laser beams, ν_1 and ν_2, the process described here seems suitable for study and comparison of the dynamics of nonlinear scattering and fluorescence in the case of resonant and near-resonant excitation. As in the case of a two-level system, side bands oscillating at $2\nu_1+\nu_2\pm\lambda_i/h$ are also predicted in the case treated here and may also be useful for the study of the dynamics of coherent excitation.

The preliminary experimental results also indicate that, with all transitions detuned from exact resonance, the mixed wave can have an intensity higher than that generated where the detunings from exact resonances in the free molecule are all zero. Since there is no exact resonance in the approach described here, it may be less sensitive to the mechanism of saturation and may correspond to a longer coherence length in the vapor. Currently, a continuosly tunable range of approximately 50 cm^{-1} (2 Å) with roughly constant output is achieved. However, because the tuning range can be further increased by tuning the second beam to a different vibrational band the mixed wave is essentially continuously tunable over several hundred Å. Because of this, ac Stark-effect-enhanced nonlinear scattering in a nearly resonant four-level system should have practical application in the efficient generation of tunable coherent light in the ultraviolet and vacuum-ultraviolet region of the spectrum.

[1]A. M. Bruevish and V. A. Khodovoi, Usp. Fiz. Nauk **93**, 71 (1967) [Sov. Phys.—Usp. **10**, 637 (1968)].

[2]B. R. Mollow, Phys. Rev. **188**, 1969 (1969).

[3]F. Shuda, C. R. Stroud, Jr., and M. Hercher, J. Phys. B **7**, L198 (1974).

[4]J. Morellec, D. Normand, and G. Petite, Phys. Rev. A **14**, 300 (1976); P. Kruit, W. R. Garrett, J. Kimman and M. J. Van der Wiel, J. Phys. B **16**, 3191 (1983); M. S. Pindzola and A. H. Glasser, Phys. Rev. A **30**, 1800 (1984).

[5]S. H. Autler and C. H. Townes, Phys. Rev. **100**, 703 (1955).

[6]F. Y. Wu, S. Ezekial, M. Ducloy, and B. R. Mollow, Phys. Rev. Lett. **38**, 1077 (1977).

[7]D. J. Harter and R. W. Boyd, IEEE J. Quantum Electron. **QE-16**, 1126 (1980); D. J. Harter, P. Narum, M. G. Raymer, and R. W. Boyd, Phys. Rev. Lett. **46**, 1192 (1981); D. J. Harter and R. W. Boyd, Phys. Rev. A **29**, 739 (1984).

[8]P. D. Kleiber, K. Burnett and J. Cooper, Phys. Rev. A **25**, 1188 (1982); G. L. Burdge and C. H. Lee, Appl. Phys. B **28**, 197

(1982).
[9]C. Cohen-Tannoudji and S. Reynaud, J. Phys. B **10**, 345 (1977); E. Coutens and A. Szoke, Phys. Rev. A **15**, 1588 (1977).
[10]R. T. Hodgson P. O. Sorokin, and J. J. Wynne, Phys. Rev. Lett. **32**, 343 (1974); F. S. Yomkins and R. Mahon, Opt. Lett. **6**, 179 (1981); F. S. Tomkins and R. Mahon, *ibid.* **7**, 304 (1982); A. Timmerman and R. Wallenstein, *ibid.* **8**, 517 (1983).
[11]C. Tai, F. W. Dalby, and G. L. Giles, Phys. Rev. A **20**, 233 (1979).
[12]C. Tai and Y. Wu (unpublished).
[13]R. S. Mulliken, J. Chem. Phys. **55**, 288 (1971).